Proceedings of the 2016 IEEE/SICE International Symposium on
System Integration, Sapporo Convention Center, Sapporo, Japan,
December 13-15, 2016

Analysis of Imitative Interactions between Humans and a Robot with a Neuro-dynamical System

Shingo Murata[1], Kai Hirano[2], Hiroaki Arie[1], Shigeki Sugano[1], and Tetsuya Ogata[2]

***Abstract*— Human communicative behavior is both dynamic and bidirectional. This study aims to analyze such behavior by conducting imitative interactions between human subjects and a humanoid robot that has a neuro-dynamical system. For this purpose, we take a robot-centered approach in which the change in robot performance according to difference in human partner is analyzed, rather than adopting the typical human-centered approach. A small humanoid robot equipped with a neuro-dynamical system learns imitative arm movement patterns and interacts with humans after the learning process. We analyze the interactive phenomena by different methods, including principal component analysis and use of a recurrence plot. Through this analysis, we demonstrate that different classes of interactions can be observed in the contextual dynamics of the neuro-dynamical system.**

I. Introduction

Analysis of human–agent interactions is one possible approach to investigation of human communicative behavior. A common approach in this research field is a *human-centered* approach (the left side of Fig. 1) in which the performance of human subjects or their impression is evaluated by considering the impact of the type of partner, such as virtual agents and embodied agents (robots) [1]. Children with autism spectrum disorder (ASD) are well-studied [2], [3] in this field and are known to prefer robots to humans for the interaction partner [4], [5]. Therefore, interactive robots are expected to be used in providing therapy to children with ASD [2] and evaluation of the children's cognitive ability such as imitation [6] and social behavior [7].

Boucenna et al. [8] recently proposed a novel research paradigm that employs a *robot-centered* approach (the right side of Fig. 1) with a machine learning method in which the performance of a robot is evaluated by considering the impact of the type of partner (i.e., of human subjects). In their experiments, a small humanoid robot equipped with a sensory-motor architecture based on a feedforward neural network (FNN) learned different static arm gestures demonstrated by several partners, including healthy adults, typically developing (TD) children, and children with ASD. The experimental results revealed that robot learning by interaction with children with ASD required a higher number of neural units than learning with the other partners did. This approach, of analyzing change from the robot perspective, rather than from the human perspective, is unique and may provide insights that are different from those found via the conventional approach. However, the study by Boucenna et al. is limited to analyzing one static characteristic (number of neural units required for learning) and misses an important characteristic of actual human communicative situations, namely, that interactions are dynamic and bidirectional [9], as explained below.

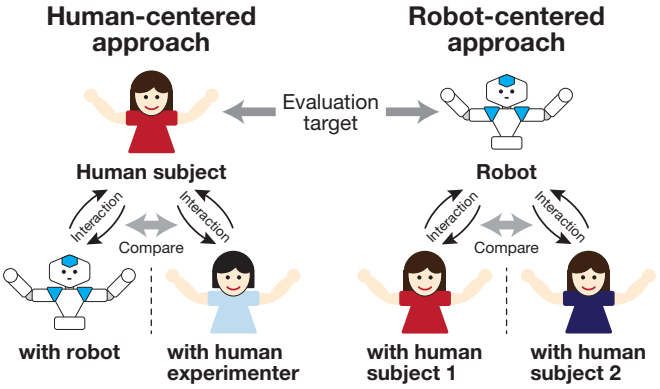

Fig. 1. Human-centered approach and robot-centered approach. In the human-centered approach, the performance of human subjects is evaluated by considering the impact of the type of partner, such as virtual agents, embodied agents (robots), and humans. In the robot-centered approach, the performance of a robot is evaluated by considering the impact of the type of partner, such as human subjects including adults, TD children, and children with ASD.

In an actual communicative situation, each person has a specific intention or plan that cannot be observed externally. These unobservable internal states are conveyed between partners by representing them in an observable way. The external representations, for example, such as gestures and/or utterances, are received as sensory (visual and/or auditory) inputs that dynamically modulate the original internal state of the receiver. Because this dynamic modulation happens bidirectionally between both partners in a spontaneous fashion, the communication converges when each internal state is well-balanced and diverges when either is unbalanced. This dynamic and bidirectional aspect needs to be considered in studies of human–robot interaction that aim to elucidate the underlying mechanism of human communicative behavior.

Ito and Tani [10] considered this aspect from a neuro-dynamical systems perspective. In their experiments, imitative interactions were carried out between a human and a small humanoid robot equipped with an extension of

This work was supported in part by a MEXT Grant-in-Aid for Scientific Research on Innovative Areas "Constructive Developmental Science" (24119003), a JSPS Grant-in-Aid for Scientific Research (S) (25220005), and the "Fundamental Study for Intelligent Machine to Coexist with Nature" program of the Research Institute for Science and Engineering, Waseda University, Japan.

[1]S. Murata, H. Arie, and S. Sugano are with the Department of Modern Mechanical Engineering, Waseda University, Tokyo, Japan.

[2]K. Hirano and T. Ogata are with the Department of Intermedia Art and Science, Waseda University, Tokyo, Japan.

978-1-5090-3329-4/16/$31.00 ©2016 IEEE

a recurrent neural network (RNN), a so-called RNN with parametric bias (RNNPB) [11]. The robot with a specific memory structure after a learning process interacted with a naïve human partner. The experimental results demonstrated coherent and incoherent dynamics of the RNNPB derived from the dynamic and bidirectional interaction with the partner. Although the study by Ito and Tani demonstrated an interesting aspect of imitative interaction, intergroup comparisons (e.g., a comparison between a group of adults and that of children) and intragroup comparisons (e.g., a comparision among subjects in a group of adults) were not considered.

We considered this background and two lines of study, typified by Boucenna et al. [8] and by Ito and Tani [10], and decided to adopt a robot-centered approach together with a neuro-dynamical system, aiming to allow comparison of human communicative behaviors. Our final project goal is to investigate intergroup and intragroup communicative differences by performing experiments involving healthy subjects and subjects with ASD. As a first step, this paper reports our developed framework and preliminary results. We performed experiments with healthy adult subjects and analyzed the contextual dynamics of the neuro-dynamical system. More specifically, we provide different analytical results in which high-dimensional contextual dynamics are projected to a low-dimensional space via principal component analysis (PCA) and as a *recurrence plot* [12] to allow visualization.

II. Methods

A. Framework for Human–robot Imitative Interactions

Figure 2 shows our developed framework, which is inspired by that in [10], for performing human–robot imitative interactions. The framework consists of three main components: a Kinect sensor (Microsoft), a humanoid robot NAO (Aldebaran Robotics), and a neuro-dynamical system. For the neuro-dynamical system, we employed a stochastic continuous-time RNN (S-CTRNN) [13]. This type of network can learn to generate predictions about the mean and variance of a target state with fluctuation. The variance-prediction mechanism enables S-CTRNNs to stably learn multiple fluctuating temporal patterns as compared with conventional CTRNNs lacking variance prediction [14]. The generation and training methods of S-CTRNN are described in the forthcoming subsections.

A robot equipped with an S-CTRNN first learned a set of behavioral patterns for the imitative interactions by integrating representations of human hand movements captured by the Kinect as visual states, robot arm movements as corresponding proprioceptive states, and contextual states in the network. For our framework in particular, the network learned to predict the mean and variance of the visuo-proprioceptive state of the robot from a received current visual state. After this learning process, the robot interacted with human subjects. During this interaction phase, the mean proprioceptive state predicted by the network was sent to the robot as a target joint angle for online control of arm movement. It should be noted that the robot behavior was based on both the past experience stored in the network as contextual states and the current situation provided to the network as visual input. This characteristic of the framework enabled the robot to perform dynamic and bidirectional interactions in which human subjects sometimes lead the interaction and the robot sometimes did.

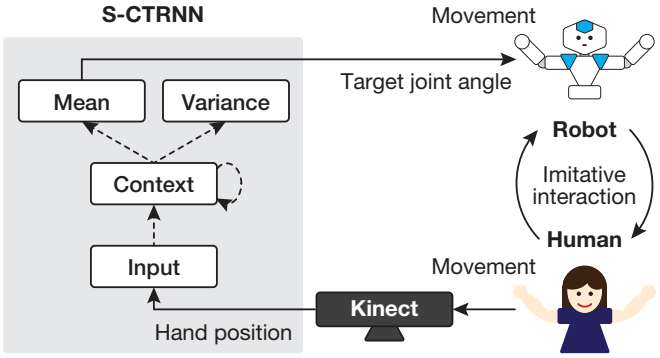

Fig. 2. Overview of framework. A Kinect, a humanoid robot, and a neuro-dynamical system (S-CTRNN) are integrated. The network receives human hand positions from the Kinect as visual input at the current time step and generates predictions about the mean and variance of visuo-proprioceptive states for the next time step. The predicted mean proprioceptive states are sent to the robot as target arm-joint angles, and the robot generates movement according to the prediction.

B. Generation Method of S-CTRNN

As shown in Fig. 2, an S-CTRNN consists of input, context, output (mean), and variance layers. In what follows, we consider estimating the mean $\boldsymbol{y}_t^{(s)}$ and variance $\boldsymbol{v}_t^{(s)}$ of an N_{O}-dimensional fluctuating target vector $\hat{\boldsymbol{y}}_t^{(s)}$ under the Gaussian assumption, where $1 \leq t$ is the time step and s is the index of time-series data items. The internal state of the ith neural unit $u_{t,i}^{(s)}$ in each layer (with the exception of the input layer) is described by

$$u_{t,i}^{(s)} = \begin{cases} \left(1 - \dfrac{1}{\tau_i}\right) u_{t-1,i}^{(s)} + \dfrac{1}{\tau_i} \left(\displaystyle\sum_{j=1}^{N_{\mathrm{I}}} w_{ij} x_{t,j}^{(s)} \right. \\ \left. + \displaystyle\sum_{j=1}^{N_{\mathrm{C}}} w_{ij} c_{t-1,j}^{(s)} + b_i \right) & (i \in I_{\mathrm{C}}), \\ \displaystyle\sum_{j=1}^{N_{\mathrm{C}}} w_{ij} c_{t,j}^{(s)} + b_i & (i \in I_{\mathrm{O}} \cup I_{\mathrm{V}}). \end{cases} \tag{1}$$

Here, I_{C}, I_{O}, and I_{V} are the index sets for the context, output, and variance layers, $x_{t,j}^{(s)}$ is the jth element of an N_{I}-dimensional input vector $\boldsymbol{x}_t^{(s)}$, $c_{t-1,j}^{(s)}$ is the jth element of an N_{C}-dimensional context vector $\boldsymbol{c}_{t-1}^{(s)}$, τ_i is the time constant of the ith context unit, w_{ij} is the synaptic weight of the connection from the jth to the ith unit, and b_i is the bias of the ith unit. In this study, the value of the initial internal state $u_{0,i}^{(s)}$ of the context units ($i \in I_{\mathrm{C}}$) was set to zero.

For the activation function of both the context and output units $\tanh(\cdot)$ was used, and for the variance unit $\exp(\cdot)$ was used.

Fig. 3. Experimental environment. The robot and a human face each other during imitative interactions.

C. Training Method of S-CTRNN

The network parameters (synaptic weights w_{ij} and biases b_i) collected in $\boldsymbol{\theta}$ are optimized to maximize the following likelihood derived from the Gaussian assumption:

$$L(\boldsymbol{\theta}) = \prod_{s=1}^{N_\mathrm{S}} \prod_{t=1}^{T^{(s)}} \prod_{i=1}^{N_\mathrm{O}} \frac{1}{\sqrt{2\pi v_{t,i}^{(s)}}} \exp\left(-\frac{(\hat{y}_{t,i}^{(s)} - y_{t,i}^{(s)})^2}{2v_{t,i}^{(s)}} \right), \tag{2}$$

where N_S is the number of time-series data items, and $T^{(s)}$ is the length of the sth data item. The parameters at learning step n ($\boldsymbol{\theta}_n$) are optimized by the gradient ascent method with a momentum term η on the log-likelihood $\ln L$:

$$\boldsymbol{\theta}_n = \boldsymbol{\theta}_{n-1} + \alpha \Delta \boldsymbol{\theta}_n, \tag{3}$$

$$\Delta \boldsymbol{\theta}_n = \frac{\partial \ln L(\boldsymbol{\theta}_{n-1})}{\partial \boldsymbol{\theta}} + \eta \Delta \boldsymbol{\theta}_{n-1}, \tag{4}$$

where α is the learning rate. The gradients $\frac{\partial \ln L(\boldsymbol{\theta})}{\partial \boldsymbol{\theta}}$ can be calculated by the conventional back-propagation through time (BPTT) method [15]. Details of the calculation of gradients are provided in [13].

D. Experimental Setup

Our experiment consisted of three phases: data recording, network training, and interaction with human subjects. Figure 3 shows the environment used during the first and third phases (data recording and interaction, respectively).

In the first phase of data recording, the robot arm movement was controlled to follow one of five predefined cyclic movements. These are shown in Fig. 4. To improve the robustness of the network, six human participants of different heights were recorded during the first phase. Among these participants, height ranged from 158 cm to 184 cm. The human participants were asked to mimic the robot's movement by moving their own arms when the robot moved its own arms. Each cyclic movement (for about 3 s) was repeated 20 times and recorded as one dataset to allow achieving a stable limit cycle attractor during the subsequent training phase. During the imitation, time-series data of the human hand positions captured by the Kinect and the robot's arm joint angles were simultaneously recoreded at a frequency of 0.1 s. This resulted in about 600 time steps, representing 60 s, for each data item. In total, $N_\mathrm{S} = 30$ data items were recorded (five movement patterns from each of the six participants). The target data recorded during this phase are 6-dimensional descriptors of human hand positions (3 elements for each hand) and 8-dimensional descriptors of robot joint angles (4 elements for each arm). The human participants from this phase did not participate in the interaction phase after the network training.

For the second phase, network training, a single network was trained on all recorded data in an offline manner. We expected that the five behavioral patterns of the robot that had been imitated by the human participants during the first phase could be embedded as multiple limit cycle attractors in the network. The numbers of input, context, output, and variance units were $N_\mathrm{I} = 6$, $N_\mathrm{C} = 30$, $N_\mathrm{O} = 14$, and $N_\mathrm{V} = 14$, respectively. The number of context units to use was experimentally determined, but the numbers of other units were determined directly from the dimensions of the visual states (considered for input, output, and variance) and proprioceptive states (considered for output and variance). Beucase the maximum value of the log-likelihood $\ln L$ depends on the total length T_total of the target data items and the dimensionality N_O of the data, the learning rate α was scaled by a parameter $\tilde{\alpha} = 0.0001$ satisfying the relation $\alpha = \frac{1}{T_\mathrm{total} N_\mathrm{O}} \tilde{\alpha}$.

In the third phase of the experiment, interaction after network training, the trained network was implemented on the robot and the robot interacted with 41 naïve human partners. None of the third-phase human partners knew in advance which behavioral patterns had been learned by the robot. They were asked to find the patterns through interacting with the robot. The human participants were informed that they needed to demonstrate cyclic arm movements and that if their movement pattern had been learned in the training phase, the robot would try to imitate their movements. Each trial of this interaction phase lasted for two minutes and four trials were conducted for each human participant. After each trial, participants were asked to identify any discovered patterns and answer a questionnaire about their impressions of the robot, the robot's movement, and the game. This was done to allow analyzing the subjective assessments of the robot by its human partners. The questionnaire was based on the semantic differential (SD) method in which 23 antonymous adjective pairs were rated from one to seven. The adjective pairs translated from Japanese words, which were determined by referring to the previous studies [16], [17], are provided in Table. I.

III. Results and Discussion

Before performing the interaction portion of the experiment, we investigated the results of network training. By employing closed-loop generation in which the visual (mean) prediction at time step t was used as the visual input at time step $t+1$, we confirmed that the network was able to autonomously recreate the learned patterns. This result

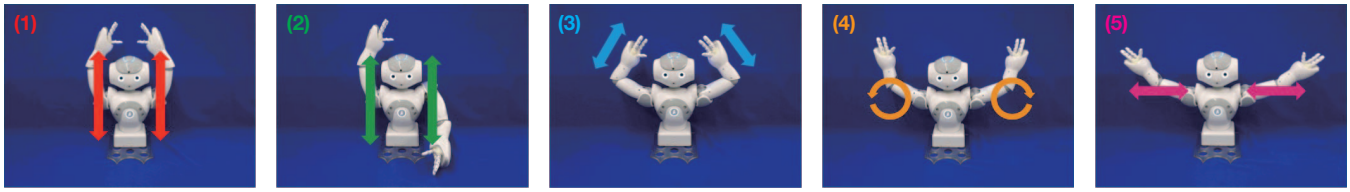

Fig. 4. The five different movement patterns designed for NAO. (1) Swinging both arms up and down in phase. (2) Swinging both arms up and down in anti-phase. (3) Moving both arms over the head. (4) Moving both arms in a circular pattern in the front of the body. (5) Moving both arms side to side in the front of the body.

TABLE I
ANTONYMOUS ADJECTIVE PAIRS IN THE QUESTIONNAIRE

No	Subject + Verb	Adjective Pairs	
1	The robot is	likable	dislikable
2	The robot is	approachable	unapproachable
3	The robot is	cheerful	awful
4	The robot is	friendly	unfriendly
5	The robot is	kind	unkind
6	The robot is	cute	hateful
7	The robot is	gentle	afraid
8	The robot is	wise	stupid
9	The robot is	familiar	unfamiliar
10	The robot's movement is	fast	slow
11	The robot's movement is	comprehensible	incomprehensible
12	The robot's movement is	active	passive
13	The robot's movement is	positive	negative
14	The robot's movement is	humanly	mechanical
15	The robot's movement is	small	large
16	The robot's movement is	sensitive	insensitive
17	The robot's movement is	smooth	rough
18	The robot's movement is	simple	complicated
19	The robot's movement is	followed	ignored
20	The game is	fun	boring
21	The game is	easy	difficult
22	The game is	successful	failed
23	The leader of the game is	me	robot

indicates that the patterns had been successfully acquired and were represented in the context states of the network as a set of multiple limit cycle attractors. To allow formal assessment, we performed PCA on the 30-dimensional contextual dynamics generated during the closed-loop testing. Figure 5 shows the first, second, and third principal components of the attractors for each pattern, grouped by color according to pattern. We can observe that for pattern (1), slight differences in demonstrations by the six human demonstrators were acquired as two similar limit cycle attractors. Patterns (4) and (5) exhibit similar results. In pattern (2), only a single limit cycle attractor was acquired from the six demonstrations; for pattern (3), in contrast, three similar limit cycle attractors were acquired.

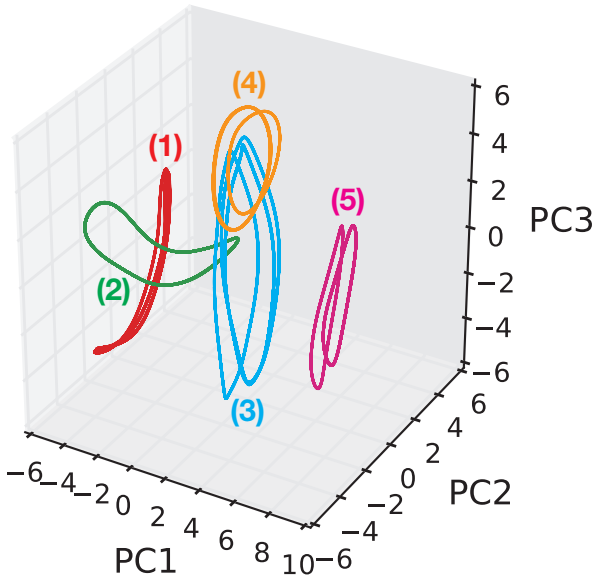

Fig. 5. Multiple limit cycle attractors acquired in the context space of the single trained network. The dimensionality of the space was reduced from 30 to 3 by applying PCA. The given index numbers correspond to those in Fig. 4. Two similar attractors were acquired for each of patterns (1), (4), and (5). A single attractor was acquired for pattern (2), and three similar attractors were acquired for the pattern (3).

We then conducted the interaction portion of the experiment, wherein human subjects interacted with a robot equipped with the network trained to have the set of multiple attractors. In what follows, we briefly review our results and then present a detailed analysis of them.

Throughout the experiment, whenever a human participant demonstrated a movement pattern known to the robot, the robot successfully imitated the demonstrated movement. However, human demonstrations of movements not learned by the robot could not be imitated by the robot, and the robot movement became unstable in such cases. Only 1 out of 41 human testers found all trained patterns, and only 1 was unable to find any patterns after four interaction trials. All other participants discovered at least one pattern.

To analyze the contextual dynamics that occurred during the interaction phase, we performed PCA of the dynamics recorded during the interaction. We also performed another analysis by using a recurrence plot [12] to visualize the recurrences of the states of the (high-dimensional) dynamical system within a two-dimensional space. A recurrence plot can be obtained for the high-dimensional dynamical system

in the following way.

1) Compute the Euclidean distance d between the 30-dimensional context state vector at time step t ($\boldsymbol{c}_t$) and that at time step t' ($\boldsymbol{c}_{t'}$), then divide the obtained distance by the number of context units (here, $N_{\mathrm{C}} = 30$) for scaling.
2) If the divided distance is less than a threshold, set here as $b = 0.1$ (i.e., if $d/N_{\mathrm{C}} < b$), plot a point at the position $(t,\ t')$ in a two-dimensional space, where both axes are time.

We can expect that when the context states during the interaction are in a limit cycle attractor with a specific period, this computational method will produce diagonal lines as the recurrence plot.

Figure 6 shows representative examples of time-series data during the interaction phase and visualized contextual dynamics. Time-series data include visual input (first row), proprioceptive prediction (second row), and context state (third row). Contextual dynamics are visualized through PCA (fourth row) and by recurrence plot (fifth row). The first example (left panels) demonstrates the transition among patterns, during which Subject A found movements in the sequence (2), (5), (4). This transition is exhibited in both the PCA visualization and the recurrence plot. Within the recurrence plot, we can see three diagonal structures, each of which corresponds one pattern in the sequence (2), (5), and (4). The second example (center panels) demonstrates repetition of a specific pattern. In this case, Subject B continued pattern (2) from the beginning to the end of the trial. The third example shown (right panels) in the right demonstrates a failed exploration, in which Subject C tried to discover a learned movement but did not find any patterns.

In addition to the above, we found a correlation between some subjective feelings about the robot during the interaction (as revealed in the questionnaire) and the experienced recurrence rate. The recurrence rate is the percentage of recurrence points (black dots) in a plot, and a higher rate indicates that the contextual states during the interaction were in one of the acquired stable attractors. The subjective feelings that exhibited correlation with recurrence rate are approachability ($r = 0.405$), kindness ($r = 0.419$), and gentleness ($r = 0.422$). These results imply that it is possible to build a bridge between subjective assessment (e.g., feelings) and objective assessment (e.g., contextual dynamics of the network implemented on the robot during the interaction).

IV. Conclusions

In this study, we considered taking the robot-centered approach to analyze human communicative behavior, and specifically imitative interactions. We developed a framework that integrates a Kinect sensor, the NAO robot, and an S-CTRNN as a neuro-dynamical system. Using the developed framework, we performed an experiment on the interaction between the trained robot and adult human subjects. Our experimental results demonstrated that different classes of imitative interactions can be visualized via both PCA and recurrence plot. The current experiment used only healthy participants. Our next step is to include participants with ASD and to investigate intergroup and intragroup differences in results.

References

[1] K. M. Lee, Y. Jung, J. Kim, and S. R. Kim, "Are physically embodied social agents better than disembodied social agents?: The effects of physical embodiment, tactile interaction, and people's loneliness in humanrobot interaction," *International Journal of Human-Computer Studies*, vol. 64, no. 10, pp. 962–973, oct 2006.

[2] K. Dautenhahn and I. Werry, "Towards interactive robots in autism therapy: Background, motivation and challenges," *Pragmatics & Cognition*, vol. 12, no. 1, pp. 1–35, 2004.

[3] S. Boucenna, A. Narzisi, E. Tilmont, F. Muratori, G. Pioggia, D. Cohen, and M. Chetouani, "Interactive Technologies for Autistic Children: A Review," *Cognitive Computation*, vol. 6, no. 4, pp. 722–740, dec 2014.

[4] B. Robins, K. Dautenhahn, and J. Dubowski, "Does appearance matter in the interaction of children with autism with a humanoid robot?" *Interaction Studies*, vol. 7, no. 3, pp. 509–542, 2006.

[5] A. C. Pierno, M. Mari, D. Lusher, and U. Castiello, "Robotic movement elicits visuomotor priming in children with autism," *Neuropsychologia*, vol. 46, no. 2, pp. 448–454, 2008.

[6] N. Bugnariu, C. Young, K. Rockenbach, R. M. Patterson, C. Garver, I. Ranatunga, M. Beltran, N. Torres-Arenas, and D. Popa, "Human-robot interaction as a tool to evaluate and quantify motor imitation behavior in children with Autism Spectrum Disorders," in *2013 International Conference on Virtual Rehabilitation (ICVR)*. IEEE, aug 2013, pp. 57–62.

[7] J. Wainer, B. Robins, F. Amirabdollahian, and K. Dautenhahn, "Using the Humanoid Robot KASPAR to Autonomously Play Triadic Games and Facilitate Collaborative Play Among Children With Autism," *IEEE Transactions on Autonomous Mental Development*, vol. 6, no. 3, pp. 183–199, sep 2014.

[8] S. Boucenna, S. Anzalone, E. Tilmont, D. Cohen, and M. Chetouani, "Learning of Social Signatures Through Imitation Game Between a Robot and a Human Partner," *IEEE Transactions on Autonomous Mental Development*, vol. 6, no. 3, pp. 213–225, sep 2014.

[9] U. Hasson and C. D. Frith, "Mirroring and beyond: coupled dynamics as a generalized framework for modelling social interactions," *Philosophical Transactions of the Royal Society B: Biological Sciences*, vol. 371, no. 1693, p. 20150366, may 2016.

[10] M. Ito and J. Tani, "On-line Imitative Interaction with a Humanoid Robot Using a Dynamic Neural Network Model of a Mirror System," *Adaptive Behavior*, vol. 12, no. 2, pp. 93–115, jun 2004.

[11] J. Tani, "Learning to generate articulated behavior through the bottom-up and the top-down interaction processes." *Neural Networks*, vol. 16, no. 1, pp. 11–23, jan 2003.

[12] J.-P. Eckmann, S. O. Kamphorst, and D. Ruelle, "Recurrence Plots of Dynamical Systems," *Europhysics Letters (EPL)*, vol. 4, no. 9, pp. 973–977, nov 1987.

[13] S. Murata, J. Namikawa, H. Arie, S. Sugano, and J. Tani, "Learning to Reproduce Fluctuating Time Series by Inferring Their Time-Dependent Stochastic Properties: Application in Robot Learning Via Tutoring," *IEEE Transactions on Autonomous Mental Development*, vol. 5, no. 4, pp. 298–310, dec 2013.

[14] S. Murata, H. Arie, T. Ogata, J. Tani, and S. Sugano, "Learning and Recognition of Multiple Fluctuating Temporal Patterns Using S-CTRNN," in *Artificial Neural Networks and Machine Learning ICANN 2014*, 2014, pp. 9–16.

[15] D. E. Rumelhart, G. E. Hinton, and R. J. Williams, "Learning internal representations by error propagation," in *Parallel Distributed Processing: Explorations in the Microstructure of Cognition*, D. E. Rumelhart and D. McClelland, Eds. Cambridge, MA: The MIT Press, 1986, pp. 318–362.

[16] T. Kanda, H. Ishiguro, and T. Ishida, "Psychological analysis on human-robot interaction," *International Conference on Robotics and Automation*, vol. 4, pp. 4166–4173, 2001.

[17] Y. Kondo, K. Takemura, J. Takamatsu, and T. Ogasawara, "A Gesture-Centric Android System for Multi-Party Human-Robot Interaction," *Journal of Human-Robot Interaction*, vol. 2, no. 1, pp. 133–151, 2013.

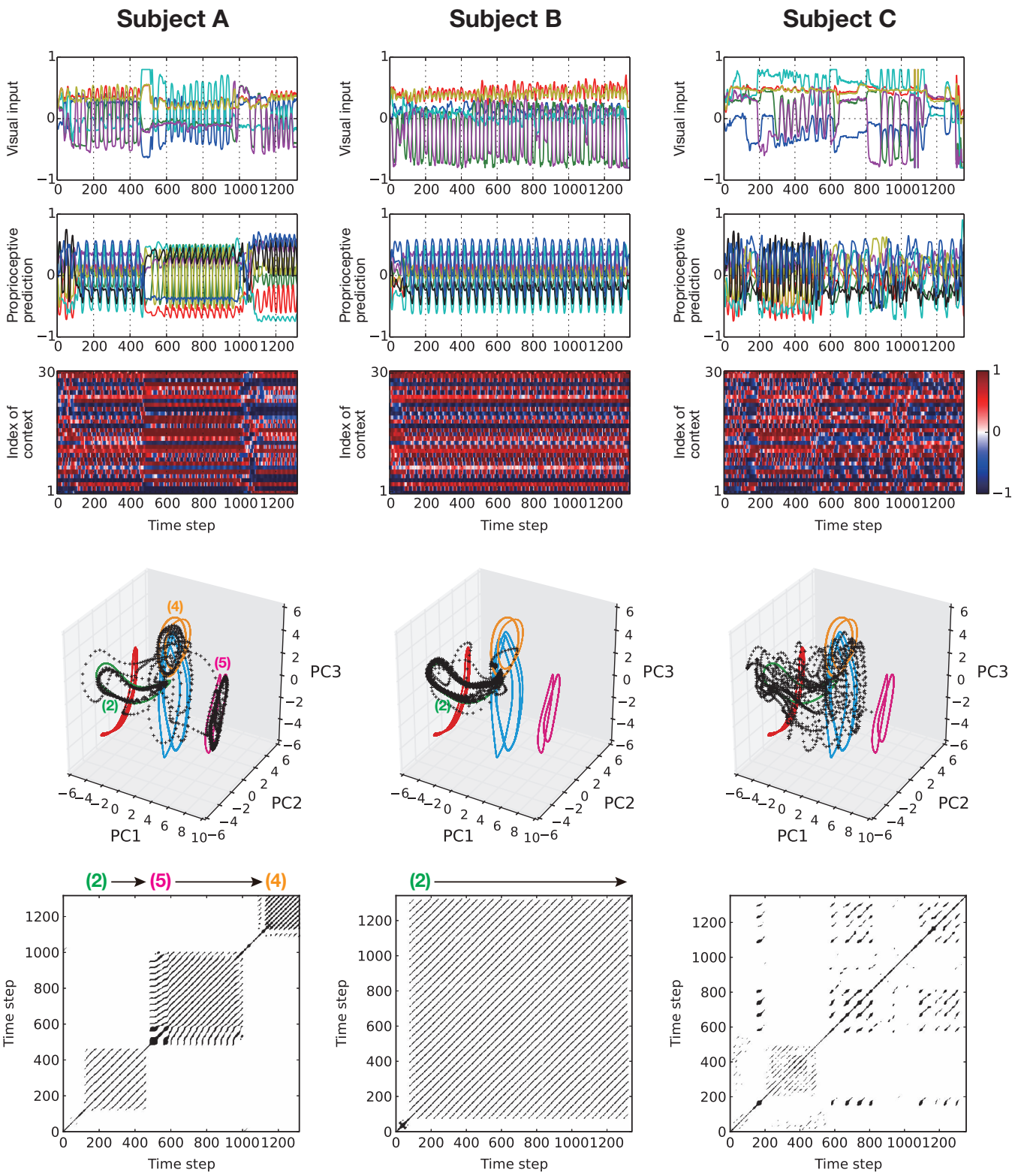

Fig. 6. Time-series data and visualized contextual dynamics for three representative situations during the interaction phase. Time-series data include visual input (first row), proprioceptive prediction (second row), and context state (third row). Contextual dynamics are visualized through PCA (fourth row) and recurrence plot (fifth row). In the panels of PCA, the states during the interaction phase are marked by "+" symbols. The set of multiple limit cycle attractors (as found by the closed-loop generation shown in Fig. 5) are included for comparison. Subject A found patterns (2), (5), and (4) in that order during the visualized trial. Subject B repeated the pattern (2) after finding it. Subject C did not find any pattern during the visualized trial. In the PCA space, we can see dense grouping of the points for Subjects A and B. These dense parts correspond to the acquired attractors. In the panels of the recurrence plots, we can see three diagonal structures for Subject A and one for Subject B. Each pattern corresponds to an attractor shown in the upper panel. These structures represent the periodical characteristic of internal neural dynamics.